

# Mott and band-insulator transitions in the binary-alloy Hubbard model: Exact diagonalization and determinant quantum Monte Carlo simulations

N. Paris, A. Baldwin, and R. T. Scalettar

*Physics Department, University of California, Davis, California 95616, USA*

(Received 20 September 2006; published 19 April 2007)

We use determinant quantum Monte Carlo simulations and exact diagonalization to explore insulating behavior in the Hubbard model with a bimodal distribution of randomly positioned local site energies. From the temperature dependence of the compressibility and conductivity, we show that gapped, incompressible Mott insulating phases exist away from half-filling when the variance of the local site energies is sufficiently large. The compressible regions around this Mott phase are metallic only if the density of sites with the corresponding energy exceeds the percolation threshold, but are Anderson insulators otherwise.

DOI: [10.1103/PhysRevB.75.165113](https://doi.org/10.1103/PhysRevB.75.165113)

PACS number(s): 71.10.Fd, 02.70.Uu, 71.30.+h, 75.10.Nr

## INTRODUCTION

The translationally invariant Hubbard model has long been studied as a model of itinerant magnetism and (Mott) insulating behavior. More recently, the possibility of unconventional (*d*-wave) superconductivity and spontaneously occurring charge inhomogeneities (stripes and checkerboards) has been explored, especially in the context of high-temperature superconductivity.<sup>1</sup> Including disorder in the Hubbard Hamiltonian—for example, in the form of a distribution of bond or site energies—imposes charge inhomogeneity externally and allows for the exploration of a number of other interesting phenomena such as the formation of Anderson insulating phases, possible transitions to metallic behavior driven by interactions,<sup>2,3</sup> and the influence of disorder on magnetic correlations.<sup>4</sup>

A particularly interesting suggestion made recently<sup>5-7</sup> concerns the possibility of alloy Mott insulating phases away from half-filling in a Hubbard model corresponding to a binary alloy—that is, for which the probability distribution of site energies is bimodal,  $P(\epsilon_i) = x\delta(\epsilon_i + \Delta/2) + (1-x)\delta(\epsilon_i - \Delta/2)$ . The idea is that if  $\Delta$  is sufficiently large compared to the bandwidth  $W$ , the noninteracting density of states will be split and an insulating gap will separate two density-of-states peaks of weight  $x$  and  $1-x$ . When an on-site repulsion  $U$  is turned on, these two peaks may in turn be Hubbard split by  $U$ . Thus, in the limit  $\Delta > U > W$  one can have alloy Mott insulating phases at incommensurate densities  $\rho = x$  and  $\rho = 1+x$  which correspond to half-filling the two alloy subbands. Spectral functions for this model have been recently reported.<sup>8</sup> A further interesting aspect of these alloy Mott insulators is that they likely occur in the absence of antiferromagnetic ordering and its associated symmetry breaking, a phenomenon which complicates the metal-insulator transition in the translationally invariant Hubbard model at  $\rho = 1$ . Possible experimental realizations of the binary-alloy Hubbard Hamiltonian in two dimensions include Co-Fe monolayers.<sup>9</sup> The nature of magnetism in such systems has been explored by first-principles calculations.<sup>10</sup>

The previous studies of Mott transitions off half-filling within tight-binding models were with dynamical mean-field theory (DMFT). In this paper we will reexamine the physics of the binary-alloy Hubbard model using determinant quan-

tum Monte Carlo (DQMC) simulations and exact diagonalization. While these methods are restricted to finite-size lattices, they allow us to examine some of the aspects of the effects of randomness like Anderson localization which are not accessible with DMFT.

The specific Hamiltonian we study is

$$\hat{\mathcal{H}} = -t \sum_{\langle lj \rangle \sigma} (c_{j\sigma}^\dagger c_{l\sigma} + c_{l\sigma}^\dagger c_{j\sigma}) + U \sum_l n_{l\uparrow} n_{l\downarrow} + \sum_l (\epsilon_l - \mu)(n_{l\uparrow} + n_{l\downarrow}).$$

Here  $c_{l\sigma}^\dagger$  ( $c_{l\sigma}$ ) is the usual fermion creation (destruction) operator for spin  $\sigma$  on site  $l$ ,  $n_{l\sigma} = c_{l\sigma}^\dagger c_{l\sigma}$  is the number operator, and  $\langle lj \rangle$  refers to near-neighbor pairs on a two-dimensional square lattice.  $t$ ,  $\mu$ , and  $U$  are the electron hopping, chemical potential, and on-site interaction strength, respectively, and  $\epsilon_l$  is a local site energy given by the bimodal distribution described previously. The bandwidth is  $W = 8t$  when  $\Delta = U = 0$ .

This paper is organized as follows: We will first describe some of the details of our computational methodology. We then show results for the density as a function of chemical potential which illustrate the appearance of alloy Mott plateaus off half-filling and also demonstrate the consistency of DQMC simulations and direct diagonalization. Results for the participation ratio in the noninteracting limit suggest that the alloy Mott plateaus at  $\rho = x$  and  $\rho = 1+x$  could in fact be rather different, a conclusion which we then confirm by calculating the temperature dependence of the conductivity. Finally, we examine the critical hopping  $t_c$  required to destroy the alloy Mott plateau. We conclude by constructing the corresponding phase diagram.

## COMPUTATIONAL METHODS

We study the alloy Hubbard Hamiltonian with exact diagonalization and DQMC simulations.<sup>11</sup> The former approach is a standard application of the Lanczos algorithm to determine exactly the ground-state wave function. We use  $N = 8$  site lattices. This method produces exact values for the correlation functions of interacting quantum systems at  $T = 0$ . A select set of basis vectors is constructed by the repeated application of the Hamiltonian and orthogonalization

to preceding basis vectors in order to approximate the Hilbert space of the system. The power of the approach is that the ground-state wave function can be accurately captured as a linear combination of a relatively small number of vectors, typically  $O(10^2)$ , even when the system's Hilbert space dimension is  $O(10^6)$  or larger. Convergence to the ground state is verified by ensuring measurements are stable even as additional basis vectors are added.<sup>15</sup>

In this case,  $N$  is sufficiently small that we can sum over all disorder realizations. In order to reduce finite-size effects, we employ the boundary condition averaging method.<sup>12</sup> In the noninteracting limit, averaging over different hopping phases at the boundary for a finite lattice reproduces the thermodynamic limit spectrum exactly. For  $U$  nonzero, the finite-size effects, while not eliminated, are reduced.<sup>13</sup> Specifically, we implement a  $2 \times 4$  cluster with two boundary phases ( $\phi_x$  and  $\phi_y$ ), one boundary phase for each of the two independent, orthogonal boundaries. An average over the phase-space area encompassed by  $\phi_x = \{0, 2\pi\}$  and  $\phi_y = \{0, 2\pi\}$  was done by selecting 10–100  $(\phi_x, \phi_y)$  pairs.

In the DQMC approach, the partition function  $Z$  is expressed as a path integral by discretizing the inverse temperature  $\beta$ . The on-site interaction is then replaced by a sum over a discrete Hubbard-Stratonovich field.<sup>14</sup> The resulting quadratic form in the fermion operators can be integrated out analytically, leaving an expression for  $Z$  in terms of a sum over all values of the Hubbard-Stratonovich field with a summand (Boltzmann weight) which is the product of the determinants of two matrices (one for spin up and one for spin down). The sum is sampled stochastically using the Metropolis algorithm. We present results for  $6 \times 6$  lattices. We average over 5–10 realizations of the local site energies. For this lattice size, fluctuations of the results from realization to realization are roughly the same size as statistical error bars from the Monte Carlo sampling.

Equal-time operators such as the density and energy are measured by accumulating appropriate elements of the inverse of matrices  $M_\sigma$  whose determinants give the Boltzmann weight. Specifically, after the fermions are integrated out,  $\langle c_{j\sigma} c_{l\sigma}^\dagger \rangle = G_{jl\sigma}$  where  $G_\sigma = M_\sigma^{-1}$ . Two particle correlation functions are obtained from products of elements of  $G$ . For example, the correlation between spin on sites  $n$  and  $n+l$  is given by  $c_{\text{spin}}(l) = \langle S_{n+l}^- S_n^+ \rangle = \langle c_{n+l, \downarrow}^\dagger c_{n+l, \uparrow} c_{n, \uparrow}^\dagger c_{n, \downarrow} \rangle = \langle G_{n+l, n, \uparrow} G_{n, n+l, \downarrow} \rangle$ . These expectation values capture the physics exactly on the finite lattice being simulated (apart from the statistical errors arising from the sampling and “Trotter errors” arising from the discretization of  $\beta$ ). We have chosen the discretization mesh so that these Trotter errors are smaller than the statistical ones.<sup>16,17</sup>

For the conductivity  $\sigma_{\text{dc}}$ , we employ an approximate procedure<sup>19</sup> which allows  $\sigma_{\text{dc}}$  to be computed from the wave-vector  $\mathbf{q}$ - and imaginary-time  $\tau$ -dependent current-current correlation function  $\Lambda_{xx}(\mathbf{q}, \tau)$  without the necessity of performing an analytic continuation,<sup>18</sup>

$$\sigma_{\text{dc}} = \frac{\beta^2}{\pi} \Lambda_{xx}(\mathbf{q} = 0, \tau = \beta/2).$$

Here  $\beta = 1/T$  and  $\Lambda_{xx}(\mathbf{q}, \tau) = \langle j_x(\mathbf{q}, \tau) j_x(-\mathbf{q}, 0) \rangle$ , and  $j_x(\mathbf{q}, \tau)$ , the  $\mathbf{q}$ ,  $\tau$ -dependent current in the  $x$  direction, is the Fourier transform of

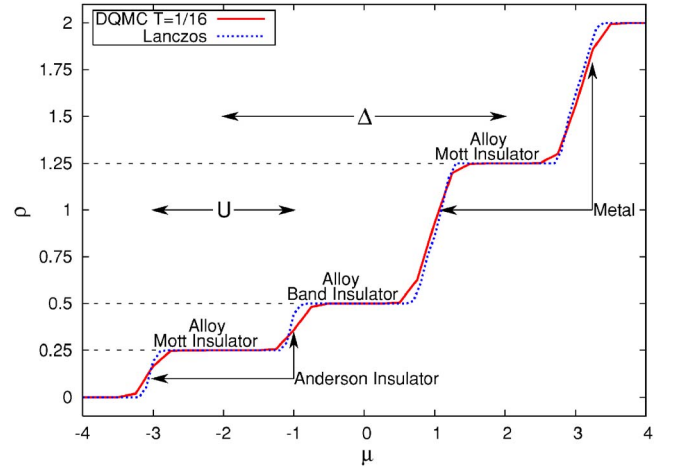


FIG. 1. (Color online) Density as a function of chemical potential for  $W=0.8$ ,  $U=2$ ,  $\Delta=4$ , and  $x=0.25$ . Solid line: ground-state exact diagonalization of an eight-site cluster. Dashed line: DQMC on  $6 \times 6$  clusters with temperature  $T=1/16$ . In the former case, results are averaged over all configurations with two sites with  $\epsilon_A = -2$  and six sites with  $\epsilon_B = +2$ , and over different choices of the boundary phases. In the latter case, results are given for a single realization. The two methods give very similar results, with the DQMC somewhat rounded by finite temperature.

$$j_x(\ell, \tau) = i \sum_{\sigma} t_{\ell+\hat{x}, \ell} e^{H\tau} (c_{\ell+\hat{x}, \sigma}^\dagger c_{\ell, \sigma} - c_{\ell, \sigma}^\dagger c_{\ell+\hat{x}, \sigma}) e^{-H\tau}.$$

This approach has been extensively tested for the superconducting-insulator transition in the attractive Hubbard model,<sup>19</sup> as well as for metal-insulator transitions in the repulsive model.<sup>2,20</sup>

In order to get further insight into the physics of Anderson localization, we also diagonalize the noninteracting system on lattices as large as  $N=64 \times 64$ . We characterize the properties of the noninteracting eigenfunctions  $|\phi_n\rangle$  through the scaling of the participation ratio,

$$\mathcal{P}_n = \left( \sum_{i=1}^N |\langle i | \phi_n \rangle|^4 \right)^{-1}.$$

For an eigenfunction perfectly localized at a site  $i_0$ ,  $\langle i | \phi_n \rangle = \delta_{i, i_0}$ , we have  $\mathcal{P}_n = 1$ , while for a perfectly delocalized eigenfunction  $\langle i | \phi_n \rangle = 1/\sqrt{N}$ , we have  $\mathcal{P}_n = N$ . In general,  $\mathcal{P}_n$  is a measure of the extent of the eigenfunction—that is, the number of sites for which  $\langle i | \phi_n \rangle$  is non-negligible.

## RESULTS

We first demonstrate the existence of the alloy Mott and band insulating phases by looking at the density as a function of chemical potential. Figure 1 shows the case  $U=2$ ,  $\Delta=4$ , and  $x=0.25$ . We see an alloy Mott insulating plateau extending from  $\mu = (-\Delta - U)/2 = -3$  to  $\mu = (-\Delta + U)/2 = -1$ , in which the total density is  $\rho = x = 0.25$ . At  $\mu = (-\Delta + U)/2 = -1$ , the lower alloy subband becomes doubly occupied and  $\rho = 2x = 0.5$ . A second plateau then reflects the “band” gap which must be surpassed to begin occupying the upper alloy sub-

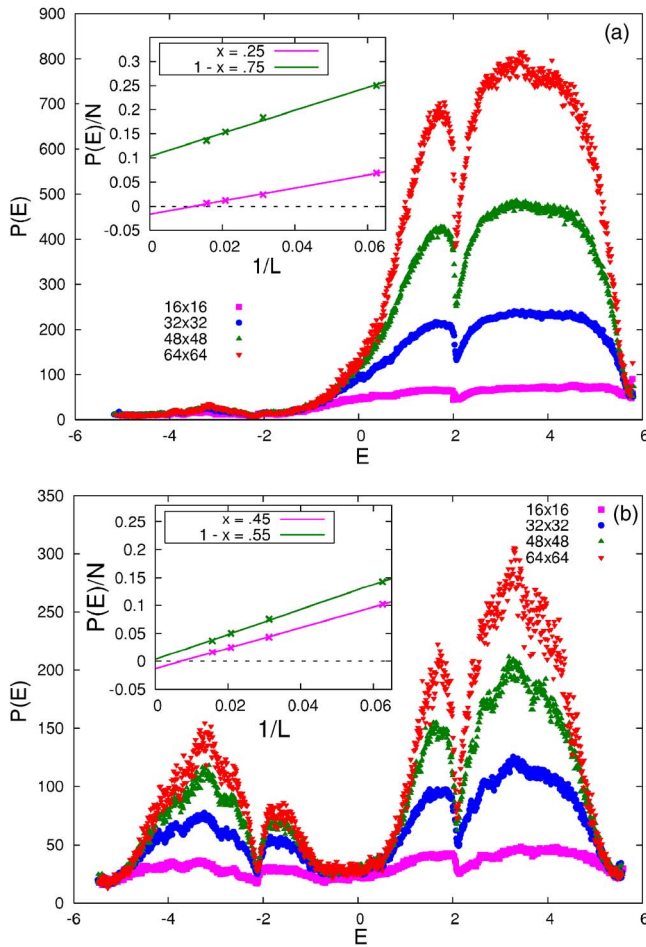


FIG. 2. (Color online) Upper panel: participation ratio  $P$  as a function of the eigenenergy  $E$  for the alloy Hubbard Hamiltonian with  $U=0$ ,  $\Delta=4$ , and  $t=1$ . Results are shown for lattice sizes varying from  $N=16 \times 16$  to  $N=64 \times 64$ .  $P(E)$  is small for the lower alloy band which has only  $x=0.25 < x_c$  of the sites, but  $P(E)$  in the upper alloy band has a significant fraction of  $N$ . The inset shows that  $P(E)/N$  scales to a nonzero value as  $N \rightarrow \infty$  for the upper band and zero for the lower band. Lower panel: the same for  $x=0.45$ . Here both alloy subbands have a density below the percolation threshold and both participation ratios scale to zero.

band, which is, like the lower subband, also Hubbard split.

In Fig. 1, the alloy Mott plateaus revealed in  $\rho(\mu)$  at  $\rho=x=0.25$  and  $\rho=1+x=1.25$  appear rather similar. We now argue that the nature of the states is, instead, quite different. For a square lattice in  $d=2$  the percolation threshold is  $x_c=0.5928$ .<sup>21</sup> We therefore might expect that the noninteracting states with site energy  $\epsilon_i=-\Delta/2=-2$ , out of which the  $\rho=x$  plateau is built, are localized, since they constitute only a fraction  $x=0.25 < x_c$  of the sites in the lattice. Meanwhile, the noninteracting states with site energy  $\epsilon_i=\Delta/2=+2$ , out of which the  $\rho=1+x$  plateau is built, are delocalized. This is illustrated in Fig. 2 where we show the participation ratio of the noninteracting system. States with energies corresponding to the upper alloy subband, which has a density exceeding the percolation threshold, extend over a macroscopic portion of the lattice. States in the lower alloy subband are localized.

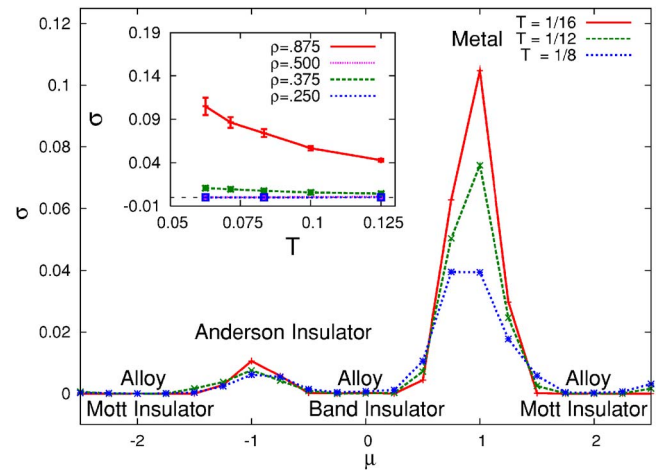


FIG. 3. (Color online) The conductivity  $\sigma_{dc}$  is shown as a function of chemical potential for several temperatures. Parameter values are as in Fig. 1. The upper alloy band, whose sites have a density larger than the percolation threshold, has a large  $\sigma_{dc}$ , which also increases as  $T$  is reduced (inset). The insulating phases have  $\sigma_{dc} \approx 0$ . The conductivity near the lower alloy subband is much smaller and much more weakly temperature dependent than the upper.

We now use the temperature dependence of the conductivity to argue that the distinction between the two alloy Mott insulating plateaus is preserved when the interaction  $U$  is turned on. Figure 3 gives  $\sigma_{dc}$  as a function of  $\mu$  for three different temperatures  $T=1/8$ ,  $T=1/12$ , and  $T=1/16$ . The conductivity is zero in both the alloy Mott- and band-insulator phases. In the regions bracketing the upper alloy band,  $\sigma_{dc}$  is relatively large and increases as  $T$  is lowered. That is, these regions are metallic. While we cannot rule out the possibility that the phase at densities bracketing the lower alloy subband is a dirty metal as opposed to an insulator,  $\sigma_{dc}$  is a factor of 10 smaller and increases much less noticeably as  $T$  is lowered. Because of the sign problem, we are not able to obtain data for lower  $T$ . However, in light of our participation ratio results, we believe that, as in the case of the Hubbard model with random site or bond energies,<sup>2,20</sup> the conductivity will turn over and decrease as  $T$  is lowered further, reflecting the insulating character of the states.

The addition of impurities decreases the conductivity in the metallic regions by a factor of 2. In Fig. 4 we have doped our system away from the Mott plateaus and kept the interaction strength fixed at  $U=2$ . For the nondisordered case ( $\Delta=0$ ), we have doped our system at  $\rho=1.4$ , well into the metallic region between Mott and doubly occupied insulating phases. With disorder ( $\Delta=4$ ), scattering is inevitable and the metallic region is limited to densities  $0.5 < \rho < 1.25$  which is the expected cause of the decrease in conductivity.

We have presented DQMC results at  $U=2$ ,  $\Delta=4$  which correspond to on-site interaction and alloy-site energy separation about 2 and 4 times the bandwidth, respectively. The reason for these strong coupling values is that for larger  $t$  it is not possible to reach low enough temperatures to see clear plateaus in the density versus chemical potential plots. However, we argued that diagonalization and DQMC gave consistent results (see Fig. 1), and we will now use the former

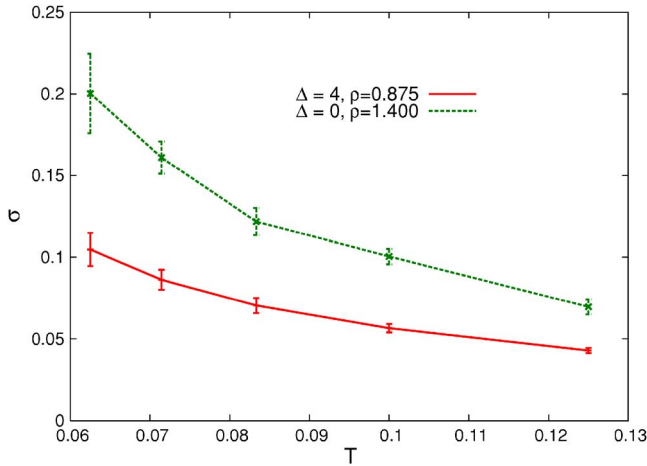


FIG. 4. (Color online) The conductivity  $\sigma_{dc}$  is shown as a function of temperature for metallic regions of different disorder with interaction energy  $U=2$ . The conductivity for the nondisordered cases is twice that of the disordered case as the insulating phases and incommensurate filling decrease the size of the metallic regions.

approach to generate the ground-state phase diagram at weaker couplings. As before, we average over different boundary condition phases to reduce finite size effects.

Figure 5 shows the length of the three plateaus as the hopping  $t$  is increased for  $U=2$ ,  $\Delta=4$ , and  $x=0.25$ . The two alloy Mott plateaus appear to vanish at roughly the same hopping strength  $t \approx 1$ . The alloy band insulator is less robust and is destroyed when quantum fluctuations are only about half as strong. The reason is that when hopping off of one of the lower-energy alloy sites for an alloy Mott insulator one has to pay a cost of  $\Delta=4$ . However, when one hops off of one of these sites for the alloy band insulator one only has to pay the cost of  $\Delta-U=2$ . This greater ease of such charge fluctuations for the alloy band insulator makes its destruction by increasing  $t$  occur earlier.

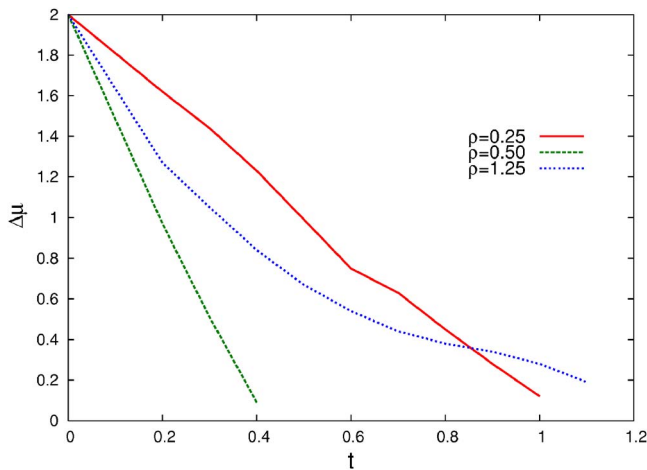


FIG. 5. (Color online) The length of the insulating plateaus,  $\Delta\mu$ , is shown as a function of hopping  $t$  for  $U=2$ ,  $\Delta=4$ , and  $x=0.25$  using exact diagonalization of  $N=8$  site clusters using boundary condition averaging. The alloy Mott-insulator plateaus at  $\rho=x$  and  $\rho=1+x$  are more robust than the alloy band-insulator plateau at  $\rho=2x$ .

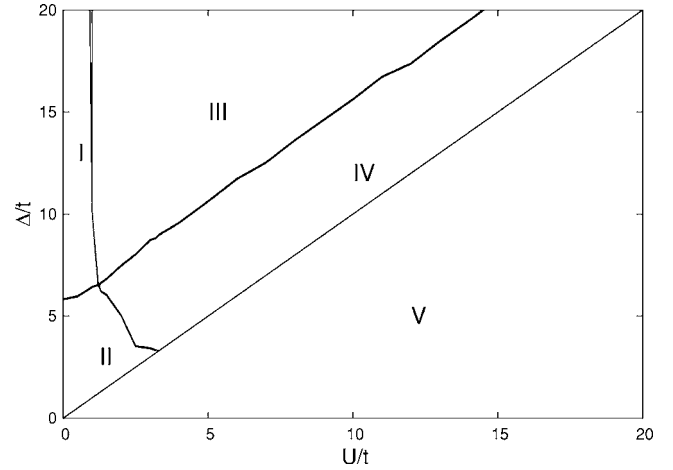


FIG. 6. Phase diagram of  $U/t$  vs  $\Delta/t$ . I: alloy band insulator at  $\rho=0.50$  and no alloy Mott insulator. II: metallic phase. III: alloy band insulator at  $\rho=0.50$  and alloy Mott insulators at  $\rho=0.25$  and  $1.25$ . IV: alloy Mott insulator at  $\rho=0.25$  and  $1.25$  and no alloy band insulator. V:  $U>\Delta$ , alloy band insulator at  $\rho=0.25$  and  $1.25$  and alloy Mott insulator at  $\rho=1.00$ .

Similar data for other choices of  $U$  and  $\Delta$  allow us to generate the ground-state phase diagram. In Fig. 6 we show four possible phases for the region of which  $U<\Delta$ . As in Fig. 5, large  $t$  which corresponds to small  $U/t$  and  $\Delta/t$  will suppress the insulating plateaus which results in a metallic phase. Taking the limiting case for small  $U/t$  and large  $\Delta/t$ , we find one alloy band insulating plateau at  $\rho=2x$ . Inversely, for small  $\Delta/t$  and large  $U/t$ , we find two alloy Mott phases at  $\rho=x$  and  $\rho=1+x$ . For large  $U/t$  and  $\Delta/t$ , both alloy band- and Mott-insulator phases coexist. The case for  $U>\Delta$  will correspond to two alloy band insulators at  $x$  and  $1+x$  and an alloy Mott insulator at half-filling for sufficiently large values of  $U/t$  and  $\Delta/t$ .

## CONCLUSIONS

In this paper we have presented DQMC and diagonalization results for the phase diagram of the Hubbard model with binary-alloy disorder. In agreement with previous treatments,<sup>5,6</sup> we find alloy Mott insulating behavior away from half-filling when the separation of the two site energies exceeds  $U$ . We extended the earlier results to characterize the nature of the compressible states above and below the alloy Mott insulating plateaus by showing that their conductivity markedly differs. Together with the results for the participation ratio, our data suggest that for  $x < x_c$  the lowest alloy Mott plateau separates two compressible Anderson insulating regions, while the upper alloy Mott plateau separates two compressible metallic phases.

Our results have focused primarily on  $x=0.25$ , but different behavior would emerge for other values of  $x$ .<sup>22</sup> For example, choosing a value of  $x=0.70 > x_c$  would not only produce alloy Mott plateaus at  $\rho=0.70$  and  $1.70$ , but also create a lower alloy Mott gap that is surrounded by metallic phases. Consequently, the upper alloy Mott gap ( $1-x=0.30 < x_c$ ) would be in between two Anderson insulating states.

This paper has explored the interplay of on-site Hubbard correlations and randomness in the form of a bimodal distribution of site energies. Related QMC studies of the effect of site and bond disorder on a strongly correlated metal<sup>2,20</sup> find that the slope  $d\sigma/dT$  can change sign from positive to negative as correlations are increased from a highly disordered noninteracting starting point, suggesting a crossover to metallic behavior. If the disorder is then increased, the sign of the slope of the conductivity can change back to positive, indicating sufficiently large disorder causing insulating behavior in a strongly correlated metal. However, the details of whether interactions and randomness cooperate or compete can depend on symmetries of Hamiltonian.<sup>20</sup>

A closer examination of magnetic correlations in this model is of interest and will be the subject of future work.

While we expect that disorder will suppress magnetism, as will the fact that the alloy Mott phases are away from commensurate fillings, it is also the case that disorder can increase the exchange constant  $J$  and hence the Néel temperature in certain circumstances.<sup>4,5,23</sup> Examining real-space magnetic correlations using DQMC would be a useful complement to previous DMFT studies.

#### ACKNOWLEDGMENTS

We acknowledge support from the National Science Foundation under Grant No. NSF ITR 0313390 and useful input from M. Lovers.

- 
- <sup>1</sup>See, for example, E. Dagotto, *Rev. Mod. Phys.* **66**, 763 (1994), and references cited therein.
- <sup>2</sup>P. J. H. Denteneer, R. T. Scalettar, and N. Trivedi, *Phys. Rev. Lett.* **83**, 4610 (1999).
- <sup>3</sup>M. Balzer and M. Potthoff, *Physica B* **359**, 768 (2005).
- <sup>4</sup>M. Ulmke, V. Janiš, and D. Vollhardt, *Phys. Rev. B* **51**, 10411 (1995).
- <sup>5</sup>K. Byczuk, M. Ulmke, and D. Vollhardt, *Phys. Rev. Lett.* **90**, 196403 (2003).
- <sup>6</sup>K. Byczuk, W. Hofstetter, and D. Vollhardt, *Phys. Rev. B* **69**, 045112 (2004).
- <sup>7</sup>M. S. Laad, L. Craco, and E. Müller-Hartmann, *Phys. Rev. B* **64**, 195114 (2001).
- <sup>8</sup>P. Lombardo, R. Hayn, and G. I. Japaridze, *Phys. Rev. B* **74**, 085116 (2006).
- <sup>9</sup>M. Pratzer and H. J. Elmers, *Phys. Rev. Lett.* **90**, 077201 (2003).
- <sup>10</sup>I. Turek, J. Kudrnovsky, V. Drchal, and P. Weinberger, *Phys. Rev. B* **49**, 3352 (1994).
- <sup>11</sup>R. Blankenbecler, D. J. Scalapino, and R. L. Sugar, *Phys. Rev. D* **24**, 2278 (1981).
- <sup>12</sup>J. Tinka Gammel, D. K. Campbell, and E. Y. Loh, Jr., *Synth. Met.* **57**, 4437 (1993).
- <sup>13</sup>C. Lin, F. H. Zong, and D. M. Ceperley, *Phys. Rev. E* **64**, 016702 (2001).
- <sup>14</sup>J. E. Hirsch, *Phys. Rev. B* **31**, 4403 (1985).
- <sup>15</sup>C. Lanczos, *J. Res. Natl. Bur. Stand.* **45**, 255 (1950).
- <sup>16</sup>R. M. Fye, *Phys. Rev. B* **33**, 6271 (1986).
- <sup>17</sup>R. M. Fye and R. T. Scalettar, *Phys. Rev. B* **36**, 3833 (1987).
- <sup>18</sup>D. J. Scalapino, S. R. White, and S. Zhang, *Phys. Rev. B* **47**, 7995 (1993).
- <sup>19</sup>N. Trivedi, R. T. Scalettar, and M. Randeria, *Phys. Rev. B* **54**, R3756 (1996).
- <sup>20</sup>P. J. H. Denteneer, R. T. Scalettar, and N. Trivedi, *Phys. Rev. Lett.* **87**, 146401 (2001).
- <sup>21</sup>D. Stauffer and A. Aharony, *Introduction to Percolation Theory* (Taylor & Francis, London, 1992).
- <sup>22</sup>A. Alvermann and H. Fehske, *Eur. Phys. J. B* **48**, 295 (2005).
- <sup>23</sup>K. Byczuk and M. Ulmke, *Eur. Phys. J. B* **45**, 449 (2005).